scientific reports

Check for updates

OPEN

Histopathological modifications and biochemical defense responses of muskmelon (*Cucumis Melo* L.) to root-knot nematode (*Meloidogyne incognita*)

V. Basavaraj[1]✉, M. S. Sharada[1], M. R. Sampathkumar[1], H. M. Mahesh[2] & A. Shanthi[3]

Root-knot nematodes (*Meloidogyne incognita*) cause significant damage to muskmelon (*Cucumis melo* L.), leading to reduced productivity. This study analysed histopathological and biochemical changes in infected plants using Scanning Electron Microscopy (SEM) and biochemical assays. Infected roots showed giant cell formation, vascular disruption, and necrosis, affecting water and nutrient transport. SEM revealed tissue depressions and deformation at nematode feeding sites. Biochemically, infection caused a decline in photosynthetic pigments—chlorophyll a (66.62%), chlorophyll b (71.94%), and total chlorophyll (65.36%). However, defense mechanisms were activated, as shown by elevated total phenol levels (114.5% in leaves, 48.92% in roots) and increased enzymatic activities. Peroxidase rose by 51.47% in leaves and 19.18% in roots, while polyphenol oxidase increased by 25.91% and 36.49%, respectively. Activities of acid phosphatase and phenylalanine ammonia-lyase also rose, indicating activation of the phenylpropanoid pathway. The study highlights *M. incognita*'s dual impact—causing structural damage while triggering plant defense—necessitating integrated pest management strategies.

Keywords Root-knot nematode, Muskmelon, Meloidogyne incognita, Histopathology, Plant defense mechanisms, Chlorophyll degradation, Biochemical responses

Muskmelon (*Cucumis melo* L.) is a widely cultivated cucurbitaceous crop, valued for its sweet and aromatic fruit. It thrives in tropical and subtropical regions, where favorable climatic conditions enable year-round cultivation[1]. Globally, muskmelon production is estimated at approximately 28.46 million tonnes[2], with India ranking third, producing 1.33 million tonnes over an area of 59,000 hectares[2]. Despite its economic significance, muskmelon production faces significant challenges due to various pests and pathogens, including bacteria, fungi, viruses, and root-knot nematodes. The increasing cultivation of muskmelon has led to concerns regarding plant health, particularly the prevalence of root diseases in major production areas[3], with root-knot nematodes being among the most destructive threats.

Root-knot nematodes (*Meloidogyne* spp.) are responsible for severe yield losses, with damage exceeding 30% in highly susceptible vegetable and fruit crops, including muskmelon[4]. Among the most common and damaging species affecting muskmelon are *M. incognita*, *M. javanica*, and *M. arenaria*[5]. These nematodes induce the formation of galls on muskmelon roots, disrupting the uptake of water and nutrients. Their impact on host plants is evident through symptoms such as root swelling, stunted growth, chlorosis, leaf curling, daytime wilting, and overall plant decline[6–8]. Due to their endoparasitic nature, root-knot nematodes persist in the soil for years, making their management challenging once they are established in agricultural fields.

Additionally, nematode-infested roots become highly susceptible to secondary infections by soil-borne pathogens. The mechanical damage caused by nematode penetration alters host physiology, creating entry points for opportunistic fungi such as Fusarium, leading to complex disease interactions that are difficult to

[1]Department of Studies in Botany, Manasagangotri, University of Mysore, Mysuru 570006, Karnataka, India. [2]Department of Botany, The Rural College, Bangalore South District, Kanakapura 562117, Karnataka, India. [3]Department of Fruit Science, Horticulture College and Research Institute, Tamil Nadu Agricultural University (TNAU), Coimbatore 641003, Tamil Nadu, India. ✉email: basavarajv@botany.uni-mysore.ac.in

manage and result in significant crop losses[6,9,10]. Considering these challenges, the present study examines the histopathological alterations in muskmelon roots infected by *M. incognita* using Scanning Electron Microscopy (SEM). Furthermore, this research aims to assess the biochemical changes induced by *M. incognita* infestation in muskmelon under controlled pot culture conditions.

Results

Histopathological changes caused by *M. incognita* through SEM analysis

Scanning Electron Microscopy (SEM) analysis of galled muskmelon root sections revealed significant ultrastructural modifications induced by *M. incognita* infection. Infected roots exhibited severe anatomical distortions, particularly in the vascular system and storage tissues, making it difficult to discern the normal vascular strand organization. SEM observations of healthy muskmelon roots confirmed typical dicot root features, including a uniseriate epidermis, parenchymatous cortex, and well-organized vascular bundles showing clear differentiation of metaxylem, protoxylem, and pith (Fig. 1-a). In contrast, nematode-infested roots displayed extensive structural damage, including epidermal and cortical deformation, vascular tissue disruption, and the presence of irregularly shaped cells and cavities in the cortex (Fig. 1-b).

The vascular region underwent severe alterations, with the epidermal layers ruptured. The stele appeared highly disorganized, forming large cavities due to the deformation of transport elements, which separated it from the cortex. Hypertrophy and hyperplasia of traumatic cells induced by nematode infection reduced the shape and thickness of the affected cortical and stelar regions. Numerous pear-shaped adult female nematodes were observed in the cortical region, embedded within traumatic cells near the root periphery (Fig. 1-c). Additionally, the formation of large, thick-walled giant cells in the damaged parenchymatous tissue was evident, with 4–6 giant cells clustered at feeding sites (Fig. 1-f).

SEM analysis also revealed localized cellular degradation at nematode feeding sites, with visible depressions indicating nematode attachment and feeding (Fig. 1-c). Cross-sectional analysis of infected roots displayed

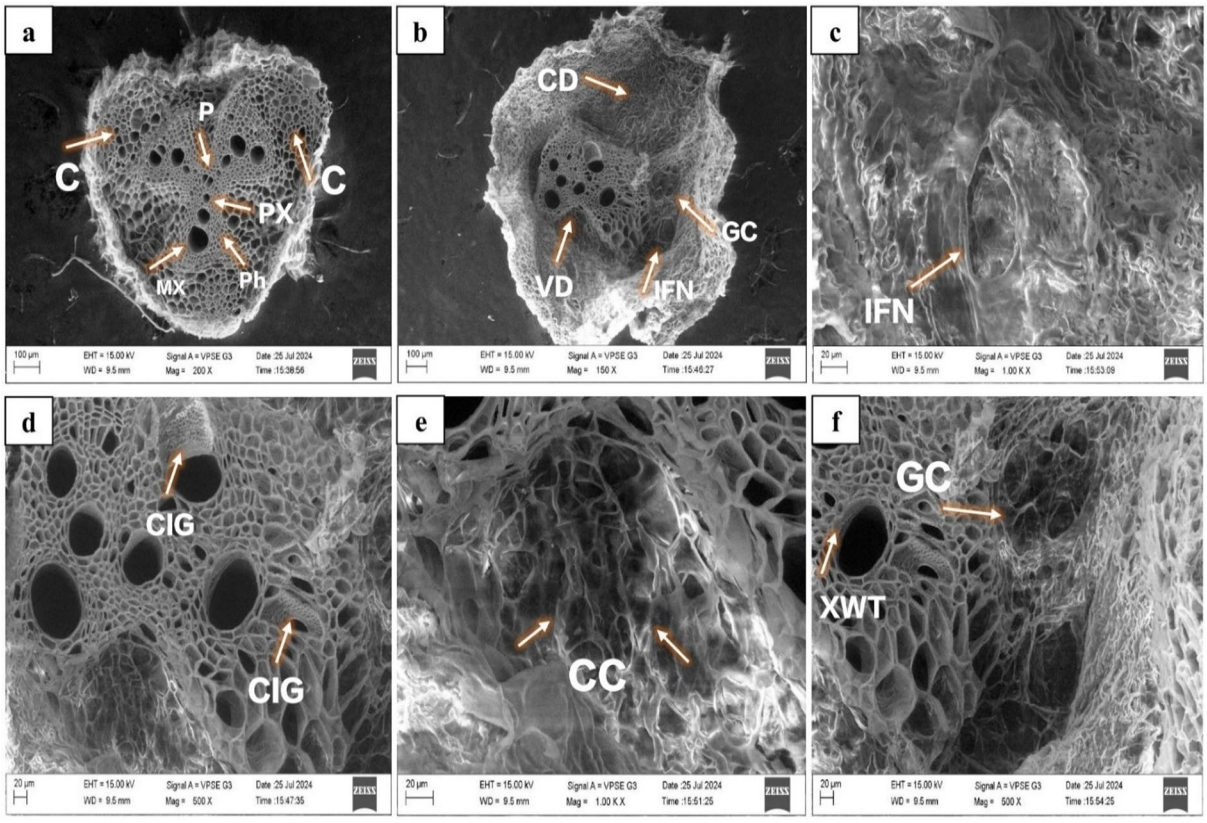

Fig. 1. Scanning Electron Microscope (SEM) images of healthy and infected root sections of Muskmelon. (a) SEM image of Muskmelon root section (Healthy) showing normal cell structures viz., C-cortex, MX-Metaxylem, PX-Protoxylem, Ph-Phloem, P-Pith. (b) SEM image of Muskmelon root section (*M. incognita* infested) showing distrupted cell structures viz., CD-Cortical distruption, VD-Vascular distruption, GC-Giant cells, IFN-Impression of female nematode. (c) SEM image of Muskmelon root section (*M. incognita* infested) showing the clear impression of female root-knot nematode (IFN). (d) SEM image of Muskmelon root section (*M. incognita* infested) showing the cellular ingrowth (CIG). (e) SEM image of Muskmelon root section (*M. incognita* infested) showing the coalsed cellular (CC) structures in the cortical region. (f) SEM image of Muskmelon root section (*M. incognita* infested) showing the Xylem wall thickening (XWT) and Giant cells (GC).)

cell wall dissolution (Fig. 1-e), cellular ingrowth (Fig. 1-d), and xylem wall thickening (XWT) (Fig. 1-f), likely a consequence of nematode-induced enzymatic activity. The development of reticulate cell wall ingrowths adjacent to xylem elements was particularly notable, with an increased ingrowth density correlating with the extent of giant cell formation (Fig. 1-d). This structural modification potentially impairs vascular function, leading to embolism, where excessive xylem tension results in air and water vapor accumulation, disrupting water transport and causing desiccation in above-ground plant parts.

Furthermore, infected roots exhibited an increased root diameter with an irregular longitudinal cell arrangement, and female nematodes were found adhering to affected areas. The presence of wound-type vascular bundles, characterized by irregular cage-like xylem formations surrounding the infection sites (Fig. 1-f), was also noted. These alterations ultimately contribute to above-ground symptoms, such as stunted growth, chlorosis, and wilting of muskmelon plants. Overall, SEM analysis provided valuable insights into the ultrastructural changes associated with *M. incognita* infection in muskmelon roots, highlighting critical aspects of host-nematode interactions.

Chlorophyll content

Chlorophyll content, a crucial indicator of plant photosynthetic capacity, demonstrated a significant decline in infected muskmelon plants. Chlorophyll a in the control group averaged 0.1462 mg/g, whereas infection led to a reduction of 66.62%, with a mean value of 0.0488 mg/g. Chlorophyll b followed a similar trend, decreasing by 71.94% from 0.0606 mg/g in the control to 0.0170 mg/g in infected plants. The total chlorophyll content was reduced by 65.36%, from 0.3696 mg/g in the control to 0.1280 mg/g in the infected group. These reductions suggest a compromised photosynthetic efficiency due to nematode infection, potentially affecting the overall health and growth of the plant (Table 1 and Fig. 2-A).

Effect of *M. incognita* on biochemical parameters

Root-knot nematode (*M. incognita*) infection significantly impacts muskmelon plants, causing alterations in key physiological parameters, including chlorophyll content, phenolic compounds, and enzymatic activities. The study presents findings on these parameters in both leaves and roots, revealing notable differences between control and infected plants.

Total phenol content

In contrast to chlorophyll, total phenol content, a key marker of plant defense, increased significantly in response to nematode infection. In leaves, the total phenol content rose by 114.5%, from 0.309 µg/g in the control to 0.663 µg/g in the infected plants. Similarly, root phenol content increased by 48.92%, from 0.531 µg/g to 0.791 µg/g. These increases suggest an induced defense response, likely aimed at mitigating the damage caused by the nematode infection (Table 2 and Fig. 2-B).

Peroxidase activity (PO)

Peroxidase activity, a marker of oxidative stress and defense, was significantly higher in infected muskmelon plants. In leaves, peroxidase activity increased by 51.47%, from 1.657 min^{-1} g^{-1} in the control to 2.510 absorbance units in the infected group. Root peroxidase activity also showed a 19.18% increase, from 0.907 to 1.081 min^{-1} g^{-1}. This enhanced peroxidase activity indicates the plant's response to oxidative stress and its role in defending against the nematode invasion (Table 3 and Fig. 2-C).

Polyphenol oxidase (PPO) activity

PPO activity, involved in oxidative defense, also increased significantly in both leaves and roots following nematode infection. Leaf PPO activity increased by 25.91%, from 1.173 min^{-1} g^{-1} in the control to 1.477 min^{-1} g^{-1} in infected plants. Root PPO activity showed a more pronounced increase of 36.49%, from 0.970 to 1.324 absorbance units. These results further highlight the plant's enzymatic defense mechanisms activated during nematode stress (Table 4 and Fig. 2-D).

Acid phosphatase activity

Acid phosphatase, an enzyme associated with hydrolytic processes and phosphorus metabolism, exhibited significant increases in both leaves and roots of infected muskmelon. Leaf acid phosphatase activity increased by 19.04%, from 1.050 to 1.250 m mol p-nitrophenol mg^{-1} protein min^{-1}, while root activity rose by 25.02%,

	Chlorophyll content mg/g (Mean ± SE)		
(a) Treatment	Chlorophyll-a	Chlorophyll-b	Total chlorophyll
Control	0.1462 ± 0.0026	0.0606 ± 0.0022	0.3696 ± 0.0037
Infected	0.0488 ± 0.0016 (-66.62%)	0.0170 ± 0.0008 (-71.94%)	0.1280 ± 0.0015 (-65.36%)
SE(d)	0.00345	0.00268	0.00450
CD	0.00181	0.00140	0.00236

Table 1. Effect of root-knot nematode *M. incognita* on chlorophyll (a, b and total) contents in Muskmelon. Each value is an average of five replications, SE – Standard error, SE(d) - Standard Error of Difference, CD - Critical Difference. Values given in the parentheses represent the percent reduction in chlorophyll content.

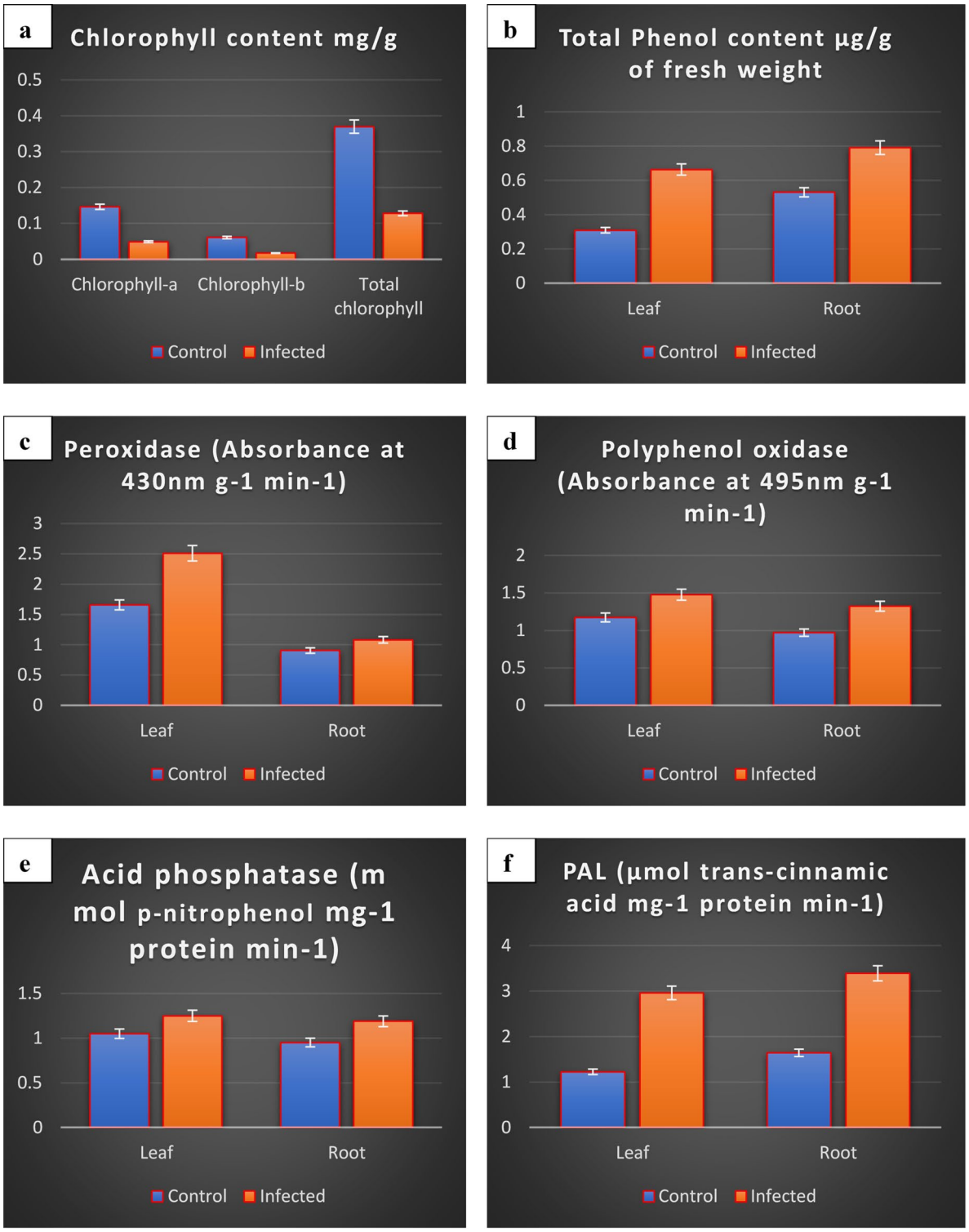

Fig. 2. Biochemical analysis of muskmelon under control and nematode-infected conditions. The graphs illustrate variations in (a) Chlorophyll content, (b) Total Phenol content, (c) Peroxidase activity, (d) Polyphenol Oxidase (PPO) activity, (e) Acid Phosphatase activity, and (f) Phenylalanine Ammonia Lyase (PAL) activity. Notable decreases in chlorophyll content and increases in phenol, peroxidase, PPO, acid phosphatase, and PAL activities were observed in infected plants compared to controls, indicating stress responses triggered by nematode infection.

Treatment	Total Phenol content µg/g of fresh weight	
	Leaf	Root
Control	0.309 ± 0.003	0.531 ± 0.004
Infected	0.663 ± 0.003 (+ 114.5%)	0.791 ± 0.002 (+ 48.92%)
SE(d)	0.004	0.004
CD	0.009	0.010

Table 2. Effect of root-knot nematode *M. incognita* on total phenol content in Muskmelon. Each value is an average of five replications, SE – Standard error, SE(d) - Standard Error of Difference, CD - Critical Difference. Values given in the parentheses represent the percent increase in total phenol content.

Treatment	Peroxidase (absorbance at 430 nm g^{-1} min^{-1})	
	Leaf	Root
Control	1.657 ± 0.018	0.907 ± 0.002
Infected	2.510 ± 0.014 (+ 51.47%)	1.081 ± 0.008 (+ 19.18%)
SE(d)	0.023	0.008
CD	0.053	0.019

Table 3. Effect of root-knot nematode *M. incognita* on peroxidase activity in Muskmelon. Each value is an average of five replications, SE – Standard error, SE(d) - Standard Error of Difference, CD - Critical Difference. Values given in the parentheses represent the percent increase in peroxidase activity.

Treatment	Polyphenol oxidase (absorbance at 495 nm g^{-1} min^{-1})	
	Leaf	Root
Control	1.173 ± 0.002	0.970 ± 0.003
Infected	1.477 ± 0.006 (+ 25.91%)	1.324 ± 0.005 (+ 36.49%)
SE(d)	0.007	0.006
CD	0.016	0.014

Table 4. Effect of root-knot nematode *M. incognita* on polyphenol oxidase activity in Muskmelon. Each value is an average of five replications, SE – Standard error, SE(d) - Standard Error of Difference, CD - Critical Difference. Values given in the parentheses represent the percent increase in Polyphenol oxidase activity.

from 0.951 to 1.189 m mol p-nitrophenol mg^{-1} protein min^{-1}. These increases indicate an enhanced hydrolytic enzyme response as part of the plant's defense strategy against nematode infection (Table 5 and Fig. 2-E).

Phenylalanine ammonia lyase (PAL) activity

The phenylpropanoid pathway, as evidenced by PAL activity, was also activated in response to nematode infection. In leaves, PAL activity increased by 141.74%, from 1.224 µmol trans-cinnamic acid mg^{-1} protein min^{-1} to 2.959 µmol. Similarly, root PAL activity increased by 106.64%, from 1.641 to 3.391 µmol. These substantial increases suggest that the plant is activating the phenylpropanoid pathway, which is crucial for producing secondary metabolites that aid in defense (Table 6 and Fig. 2-F).

Discussion

The histopathological analysis of muskmelon roots infected with *Meloidogyne incognita* using Scanning Electron Microscopy (SEM) revealed extensive tissue disorganization, particularly in the vascular and storage tissues. Cortical deformation, vascular disruption, and irregular cellular structures were prominent, highlighting the nematode's detrimental effects on the host root system. Pear-shaped female nematodes embedded near the root periphery suggest their exploitation of host tissues to establish feeding sites, a crucial strategy for survival and reproduction. Similar results were observed by Shandeep et al.[11] in okra plant infested by *M. incognita*. These feeding sites disrupt root physiology, impeding nutrient and water uptake, leading to plant decline. Present findings corroborate the findings of Rani and Kumari[12] in Mulberry roots infested by *M. incognita*.

SEM offers detailed topographic insights into structural alterations caused by nematode infection, with a resolution of at least 10 nm[13]. Nematode-infected root parenchyma cells enlarge, dissociate, and displace around

Treatment	Acid phosphatase (m mol *p*-nitrophenol mg^{-1} protein min^{-1})	
	Leaf	Root
Control	1.050 ± 0.014	0.951 ± 0.007
Infected	1.250 ± 0.017 (+19.04%)	1.189 ± 0.002 (+25.02%)
SE(d)	0.022	0.007
CD	0.051	0.017

Table 5. Effect of root-knot nematode *M. incognita* on acid phosphatase activity in Muskmelon. Each value is an average of five replications, SE – Standard error, SE(d) - Standard Error of Difference, CD - Critical Difference. Values given in the parentheses represent the percent increase in Acid phosphatase activity.

Treatment	PAL (µmol trans-cinnamic acid mg^{-1} protein min^{-1})	
	Leaf	Root
Control	1.224 ± 0.010	1.641 ± 0.003
Infected	2.959 ± 0.002 (+141.74%)	3.391 ± 0.108 (+106.64%)
SE(d)	0.010	0.108
CD	0.024	0.253

Table 6. Effect of root-knot nematode *Meloidogyne incognita* on phenylalanine lyase activity in Muskmelon. Each value is an average of five replications, SE – Standard error, SE(d) - Standard Error of Difference, CD - Critical Difference. Values given in the parentheses represent the percent increase in Phenylalanine lyase activity.

the root surface, preceding the secretion of the gelatinous matrix, likely driven by nematode-induced enzymatic or hormonal changes[13]. Secondary wall ingrowths within giant cells function as metabolic "sinks," promoting nutrient accumulation for nematode sustenance. Cytoplasmic contents obscuring inner cell walls were also noted, consistent with previous reports[14].

Further supporting the role of SEM in nematology, Uematsu et al.[15] documented nematode aggregation on Indian lotus roots, emphasizing structural alterations induced by nematodes. Similarly, Siddiqui et al.[16] observed tissue disorganization in the stelar region, making it difficult to identify normal root tissues, aligning with the present study's findings of severe tissue disruption affecting the endodermis, pericycle, xylem, and phloem. Feeding activity displaces vascular strands, forming abnormal vessel elements in the vascular cylinders, consistent with observations by Krusberg and Nielson[17] and Goellner et al.[18].

The formation of giant cells in cortical and pericycle regions, coupled with hyperplasia and hypertrophy, corroborates these findings. Giant cells, with thickened cell walls and enhanced metabolic activity, act as specialized feeding sites that deprive the plant of essential nutrients[11]. The presence of wound-type vascular bundles and xylem wall thickening (XWT) suggests an induced defense mechanism to restrict nematode movement. However, these modifications may also impair vascular function, leading to embolism and reduced water transport, manifesting as chlorosis and wilting[11].

Nematode-induced vascular changes play a key role in nutrient supply to the parasite, as giant cells disrupt both cortical and vascular regions[19]. Abnormal xylem vessels, often disconnected, further impair water and nutrient transport, compounding plant stress[20]. Robah et al.[21] reported that galled roots frequently exhibit distorted xylem vessels, a major symptom of nematode infection. These disruptions contribute to plant stunting and reduced vigor, underscoring the severity of nematode infestation on muskmelon roots.

Biochemical analysis further supports the detrimental effects of *M. incognita* infection on muskmelon physiology. A significant reduction in chlorophyll content, particularly chlorophyll a and chlorophyll b, indicates impaired photosynthetic capacity, likely due to vascular dysfunction that affects nutrient and water transport and damages chloroplast integrity. This decline in chlorophyll content is consistent with similar observations in nematode-infected ridge gourd and cucumber plants, further emphasizing the commonality of physiological stress induced by nematode infection[22–24].

In contrast, the observed increase in total phenolic content in infected roots and leaves suggests an induced defense response to the nematode attack. Phenolic compounds play a pivotal role in plant resistance by reinforcing cell walls, inhibiting pathogen penetration, and activating systemic defense pathways[25]. The significant upregulation of phenolic content in response to infection aligns with previous findings in resistant cultivars, where enhanced phenolic accumulation correlates with reduced nematode proliferation. The present study corroborates the findings of Rizvi and Khan[24], Mahapatra and Nayak[26], and Nayak and Pandey[27].

The elevated enzymatic activities of peroxidase (POX) and polyphenol oxidase (PPO) reinforce the plant's defensive response. POX is essential for reactive oxygen species (ROS) detoxification and lignin biosynthesis, contributing to cell wall strengthening and nematode resistance[25]. Similarly, increased PPO activity suggests

activation of oxidative defenses that disrupt nematode feeding structures, reducing the nematode's virulence. The heightened activities of acid phosphatase and phenylalanine ammonia-lyase (PAL) further emphasize an active phenylpropanoid pathway, which is critical for the biosynthesis of secondary metabolites with antimicrobial properties. Notably, the significant increase in PAL activity, particularly in roots, highlights its role in reinforcing structural barriers and limiting nematode colonization[25]. The biochemical changes in different plants infected by the root-knot nematode *M. incognita* have been reported by Chakraborty et al.[28] in tomatoes, Nikoo et al.[29] in tomatoes, Mahapatra and Nayak[26], and Ruchi and Singh[30] in bitter gourd.

These findings demonstrate the complex interaction between nematode infection and the plant's physiological responses. While *M. incognita* induces severe structural and functional damage to muskmelon roots, the plant activates a series of biochemical defense mechanisms in an attempt to mitigate the infestation's effects. However, the persistent tissue disruption and reduced photosynthetic efficiency ultimately outweigh the plant's defensive efforts, leading to reduced growth and productivity.

Conclusion

The histopathological and biochemical analyses of muskmelon roots infected with *Meloidogyne incognita* reveal significant structural and functional disruptions, including cortical deformation, vascular tissue damage, and the formation of giant cells that serve as specialized feeding sites for the nematodes. These alterations are associated with impaired nutrient and water transport, resulting in reduced plant growth and productivity. Despite the plant's defense mechanisms, such as the increased phenolic content and enzymatic activity, the nematode infestation severely affects the plant's physiological functions. Integrating resistant cultivars and nematicidal treatments could enhance muskmelon resilience and improve management strategies against root-knot nematodes.

Materials and methods

Experimental location

The study was conducted in a glasshouse at the Department of Studies in Biotechnology, Manasagangotri, University of Mysore, Mysuru, Karnataka (12.3105719° N, 76.6224571° E). Biochemical analysis and histopathological examinations of *M. incognita* infestations were performed at the Department of Studies in Botany, Manasagangotri, University of Mysore, Mysuru. The glasshouse conditions were maintained at a temperature range of 26–30 °C with a relative humidity of 70–75%.

Nematode inoculum

The root-knot nematode *M. incognita* used in this study was isolated from infected muskmelon roots. The nematodes were maintained in a glasshouse by culturing them on 14-day-old tomato (Cv. AMBER) seedlings for approximately 45 days. After this period, the nematodes were extracted by washing the roots under running tap water to remove adhering soil particles. The galled roots were then cut into sections and surface-disinfected using a 1% sodium hypochlorite (NaOCl) solution. Any residual NaOCl was eliminated through multiple rinses with sterile distilled water[31,32]. Egg masses of *M. incognita* were carefully collected using forceps under a stereo zoom microscope (Labovision AZM 100) and incubated in sterile distilled water for 48 h. After incubation, second-stage juveniles (J_2) were extracted and acclimatized for use in subsequent glasshouse experiments.

Raising of muskmelon plants

Muskmelon (Cv. Arka Siri) seeds were procured from the Indian Institute of Horticultural Sciences, Hesaraghatta, Bengaluru, India (560089). The seeds were surface-sterilized by immersing them in a 0.5% sodium hypochlorite (NaOCl) solution for 15 min, followed by thorough rinsing with distilled water. The sterilized seeds were then sown in germination trays. One week after germination, seedlings were transplanted into earthen pots (2 kg capacity) filled with a sterilized potting mixture consisting of 70% sand, 29% silt, and 1% organic matter. Each pot initially contained three seedlings, which were later thinned to a single plant per pot after seven days of establishment.

Nematode inoculation and maintenance of muskmelon plants

Freshly hatched second-stage juveniles (J_2s) of *M. incognita* were used to inoculate muskmelon plants grown in 2 kg earthen pots. Inoculation was carried out by creating four holes around the root zone of each plant, allowing direct nematode application. To facilitate nematode settlement near the plant roots, the pots were left undisturbed without watering for 24 h. Plants without nematode inoculation served as controls. The experiment followed a completely randomized design (CRD) with three replications. The plants were maintained in a glasshouse at the Department of Studies in Biotechnology, Manasagangotri, University of Mysore, Mysuru (570006), under controlled conditions: a temperature range of 26–30 °C, relative humidity of 70–75%, and a 12-hour photoperiod. Watering was done as needed to support plant growth and ensure optimal experimental conditions[22].

Histopathological studies

Preparation of root-sections

Both healthy and *M. incognita*-infected root samples were collected to examine histopathological changes. The selected roots were thoroughly washed under running water to remove adhering soil particles, ensuring high-quality sections. After cleaning, the roots were cut into small segments (1–2 cm in length) using a sterile blade. The root samples were then fixed in TAF solution for 24 h and examined under a stereo zoom microscope[33]. Selected roots, both with and without galls, were processed through an alcohol series for dehydration. Transverse sections of the roots were made via the hand sectioning method. Transverse sections were analyzed under a binocular

microscope to identify the most suitable samples for scanning electron microscopy (SEM) analysis[22]. The SEM examination was conducted to investigate the ultrastructural changes in *M. incognita*-infected muskmelon roots.

Scanning electron microscopic (SEM) studies
For Scanning Electron Microscopy (SEM), smaller transverse sections of *M. incognita*-infested and healthy (control) muskmelon roots were fixed in 2.5% glutaraldehyde prepared in 0.2 M cacodylate buffer (pH 7.2) for 2 h. The samples were then washed with cacodylate buffer, followed by double-distilled water, and subsequently dehydrated using an ethanol-acetone series. The dehydrated sections were mounted onto copper stubs using double-sided adhesive tape and coated with a 20 nm layer of gold using a sputter coater (EMS-550). The specimens were then examined under a Scanning Electron Microscope (EVO MA 15, Carl Zeiss, Germany) to observe ultrastructural changes[11–13,34]. The SEM analysis was conducted at the Institution of Excellence (IOE), Vijnana Bhavana, Manasagangotri, University of Mysore, Mysuru – 570006.

Estimation of chlorophyll content
The effect of *M. incognita* on the chlorophyll content of muskmelon was determined using the method described by Arnon[35]. One gram of finely cut fresh leaves (both healthy and nematode-infested) was ground with 20–40 mL of 80% acetone. The resulting mixture was then centrifuged at 5000–10000 rpm for 5 min. The supernatant was carefully transferred to a new container, and the centrifugation process was repeated until the residue became colorless. The absorbance of the solution was measured at 645 nm and 663 nm against an acetone blank using a Systronics UV-VIS 118 spectrophotometer. The amounts of chlorophyll a, chlorophyll b, and total chlorophyll were calculated in mg/g fresh weight using the formula provided by Arnon[35].

Biochemical studies

Estimation of total phenols
One gram of plant tissue (leaf and root samples were processed separately) was crushed in 10 mL of 20% ethanol. The mixture was spun in a centrifuge at 10,000 rpm for 15 min. The clear liquid (supernatant) collected after centrifugation was used as the enzyme extract. For the test, 0.2 mL of this extract was mixed with 3.5 mL of distilled water and 0.5 mL of Folin-Ciocalteau reagent. After waiting for 5 min, 1 mL of 20% sodium carbonate was added. After 30 min, the absorbance was read at 660 nm using a Systronics UV-VIS 118 spectrophotometer. The amount of enzyme activity was calculated and expressed as milligrams per gram of plant tissue, based on the method by Malick and Singh[36].

Estimation of peroxidase (PO)
One gram of plant tissue (leaf and root samples handled separately) was ground in 10 mL of 0.1 M phosphate buffer with a pH of 6.5. This mixture was then centrifuged at 10,000 rpm for 15 min. The clear liquid (supernatant) collected was used as the enzyme extract. For the test, 3 mL of 0.05 M pyrogallol solution was added to a test tube along with 0.1 mL of the enzyme extract. After that, 0.5 mL of 1% hydrogen peroxide was added. The absorbance change was measured immediately at 430 nm every minute using a Systronics UV-VIS 118 spectrophotometer. The enzyme activity was calculated based on how quickly the absorbance increased, and results were expressed as the rate of change per minute per milligram of protein or tissue, following the method described by Rad et al.[37].

Estimation of polyphenol oxidase (PPO)
One gram of plant tissue (leaf and root samples were treated separately) was blended with 5 mL of chilled 0.1 M sodium phosphate buffer (pH 7.0). The mixture was then centrifuged at 10,000 rpm for 20 min, and the clear liquid (supernatant) obtained was used as the enzyme extract. For the enzyme activity test, 1.5 mL of 0.1 M sodium phosphate buffer (pH 6.5) was mixed with 200 µL of the enzyme extract. The reaction was started by adding 200 µL of 0.001 M catechol. The change in absorbance was measured at 495 nm using a Systronics UV-VIS 118 spectrophotometer, with readings taken every 30 s for 5 min. The enzyme activity was calculated and reported as milligrams per gram of protein per hour, following the method of Mayer et al.[38].

Estimation of acid phosphatase
One gram of fresh plant tissue (leaf and root samples handled separately) was crushed and mixed with 10 mL of cold 50 mM citrate buffer (pH 5.3). The mixture was then centrifuged at 10,000 rpm for 10 min, and the clear liquid (supernatant) obtained was used as the enzyme extract. For the enzyme test, 3 mL of the substrate solution was first incubated at 37 °C for 5 min. After that, 0.5 mL of the enzyme extract was added, mixed thoroughly, and incubated again at 37 °C for 15 min. Once the reaction was complete, 0.5 mL of this mixture was combined with 9.5 mL of sodium hydroxide. The absorbance was then measured at 405 nm using a Systronics UV-VIS 118 spectrophotometer. Enzyme activity was calculated and reported as the amount of p-nitrophenol released per minute per milligram of protein, based on the method described by Dickerson et al.[39].

Estimation of phenylalanine ammonia lyase (PAL)
One gram of fresh plant tissue (leaf and root samples handled separately) was crushed and mixed with 10 mL of 25 mM borate-HCl buffer (pH 8.8) containing 5 mM mercaptoethanol (0.04 mL/L). The mixture was then centrifuged at 12,000 rpm for 20 min. The clear liquid (supernatant) obtained was used as the enzyme extract. In a test tube, 0.5 mL of borate buffer was combined with 0.2 mL of the enzyme extract and 1.3 mL of distilled water. The reaction was started by adding 1 mL of L-phenylalanine solution, and the mixture was incubated at 32 °C for 30 to 60 min. To stop the reaction, 0.5 mL of 1 M trichloroacetic acid was added. The absorbance was then read

at 290 nm using a Systronics UV-VIS 118 spectrophotometer. Enzyme activity was calculated as micrograms of product formed per gram of protein per minute, following the method described by Dickerson et al.[39].

Statistical analysis

Each experiment was conducted in triplicate and replicated three times. The data generated from the various experiments in the present study were analyzed using Analysis of Variance (ANOVA). The results were processed using OPSTST software, available online at CCSHAU, Hisar (www.hua.ac.in). The percentage increase and decrease in the biochemical parameters and chlorophyll indices compared to the control were calculated using the formulas provided by Irshad et al.[40] and Mukhtar et al.[41].

Data availability

The datasets analysed in this study are available from the corresponding author upon reasonable request.

Received: 5 October 2025; Accepted: 31 October 2025
Published online: 01 December 2025

References

1. Pires, M. M. M., Santos, H. A., Santos, D. F., Vasconcelos, A. S. & Aragão, C. A. Yield of muskmelon subjected to different water management with the use of polypropylene. *Horticult.Brasileira* **31**, 304–310 (2013).
2. FAOSTAT. *FAOSTAT Statistical Database* (FAO (Food and Agriculture Organization of the United Nations), 2020).
3. de Andrade, D. E., Michereff, S. J., Biondi, C. M., Nascimento, C. W. & Sales, R. Jr Freqüência de Fungos associados Ao Colapso do Meloeiro e relação com características físicas, químicas e microbiológicas Dos solos. *Summa phytopatol.* **31** (4), 327–333 (2005).
4. Sikora, R. A. & Fernandez, E. Nematode parasites of vegetables. In *Plant Parasitic Nematodes in Subtropical and Tropical Agriculture* (eds. Luc, M. et al.) 319–392 (CABI Publishing, 2005).
5. Pinheiro, J. B. & Amaro, G. B. Ocorrência e controle de nematoides nas principais espécies cultivadas de cucurbitáceas. Circular Técnica, Embrapa Hortaliças (2010). https://www.embrapa.br/busca-de-publicacoes/-/publicacao/886576/ocorrencia-e-controle-de-nematoides-nas-principais-especies-cultivadas-de-cucurbitaceas.
6. Basavaraj, V., Sharada, M. S., Sampathkumar, M. & Mahesh, H. M. Development of *Meloidogyne incognita* in muskmelon (*Cucumis Melo* L). *Ann. Agri-Bio Res.* **29** (2), 45–51 (2024a).
7. López-Gómez, M. & Verdejo-Lucas, S. Penetration and reproduction of root-knot nematodes on cucurbit species. *Eur. J. Plant. Pathol.* **138**, 863–871. https://doi.org/10.1007/s10658-013-0359-4 (2014).
8. Saha, S. S., Sinhababu, S. P. & Sukul, M. C. The effect of nematode infestation on mulberry plants and its effect on the feeding of silkworm *Bombyx Mori*. *L Nematol.* **29** (4), 463–467 (1983).
9. Dhami, D. S. et al. Characterization of multiple disease resistance in Melons (Cucumis Melo L.) against meloidogyne incognita, fusarium oxysporum, and tomato leaf curl Palampur virus. *Plant. Genet. Resourc. Charact. Utiliz.*. **22**, 27–36. https://doi.org/10.1017/S1479262123001119 (2024).
10. Francl, L. J. & Wheeler, T. A. Interaction of plant parasitic nematodes with wilt-inducing fungi. In *Nematode Interactions* (ed. Khan, M. W.) 79–103 (Springer, 1993).
11. Shandeep, S. G., Shanthi, A., Kalaiarasan, P. & Arun, A. Exploring the plant nematode interaction of meloidogyne incognita under Okra ecosystem. *Madras Agric. J.* **110** (4–6), 1. https://doi.org/10.29321/MAJ.10.200806 (2023).
12. Rani, P. & Kumari, N. V. Histopathological studies of mulberry roots infested by meloidogyne incognita (Sem analysis). *Indian J. Agricultural Res.* **57** (6), 831–835. https://doi.org/10.18805/IJARe.A-5985 (2023).
13. Wergin, W. P. & Orion, D. Scanning electron microscope study of the root-knot nematode (Meloidogyne incognita) on tomato root. *J. Nematol.* **13** (3), 358–367 (1981).
14. Jones, M. G. K. & Dropkin, V. H. Scanning electron microscopy of syncytial transfer cells induced in roots by cyst-nematodes. *Physiol. Plant Pathol.* **7** (3), 259–263 (1975).
15. Uematsu, S., Yabu, T., Yao, M., Kurihara, T. & Koga, H. Ultrastructure of early-stage infection in Browning rhizomes of Indian Lotus. *J. Nematol.* **52** (1), 1–9 (2020).
16. Siddiqui, Y., Ali, A. & Naidu, Y. Histopathological changes induced by meloidogyne incognita in some ornamental plants. *Crop Prot.* **65**, 216–220. https://doi.org/10.1016/j.cropro.2014.08.001 (2014).
17. Krusberg, L. R. & Nielsen, L. W. Pathogenesis of root-knot nematodes to the proto-rico variety of sweet potato. *Phytopathology* **48**, 30–39 (1958).
18. Goellner, M., Wang, X. & Davis, E. L. Endo-β-1,4-glucanase expression incompatible plant-nematode interactions. *Plant. Cell.* **13** (10), 2241e2255 (2001).
19. Hoth, S., Schneidereit, A., Lauterbach, C., Scholz-Starke, J. & Sauer, N. Nematode infection triggers the de Novo formation of unloading phloem that allows macromolecular trafficking of green fluorescent protein into syncytia. *Plant. Physiol.* **138**, 383–392 (2005).
20. Fester, T., Berg, R. H. & Taylor, C. G. An easy method using glutaraldehyde introduced fluorescence for the microscopic analysis of plant biotrophic interactions. *J. Microsc.* **231**, 342–348 (2008).
21. Robab, M. I., Hisamuddin, S. & Azam, T. Histopathology of roots of Glycine max (L.) Merrill was induced by root-knot nematode (Meloidogyne incognita). Arch. Phytopathol. *Plant. Prot.* **43** (18), 1758–1767 (2010).
22. Basavaraj, V. et al. Post-penetration development, pathogenicity, and histological changes in ridge gourd infected by root-knot nematode (*Meloidogyne incognita*). *Indian Phytopathol.* **77**, 1047–1056. https://doi.org/10.1007/s42360-024-00794-2 (2024).
23. Kayani, M. Z., Mukhtar, T., Hussain, M. A. & Ul-Haque, M. I. Infestation assessment of root-knot nematodes (Meloidogyne spp.) associated with cucumber in the Pothowar region of Pakistan. *Crop Prot.* **47**, 49–54 (2013).
24. Rizvi, T. F. & Khan, M. R. Biological and physiological responses of Root-knot disease development on five cucurbits exposed to different concentrations of sulfur dioxide. *Toxics* **11** (4), 334. https://doi.org/10.3390/toxics11040334 (2023).
25. Natarajan, A. et al. Standardization of the optimum effects of Indole 3-Butyric acid (IBA) to control root knot Nematode, *Meloidogyne enterolobii*, in guava (*Psidium Guajava* L). *Molecules* **28** (4), 1839. https://doi.org/10.3390/molecules28041839 (2023).
26. Mahapatra, M. & Nayak, D. K. Biochemical and physicochemical changes in susceptible and resistant bitter gourd cultivars as influenced by root knot nematode meloidogyne incognita. *J. Entom. Zool. Stud.* **7** (3), 80–87 (2019).
27. Nayak, D. K. & Pandey, R. K. Physiological and biochemical changes of susceptible and resistant Brinjal cultivars induced by root knot nematode, meloidogyne incognita. *J. Glob. Biosci.* **5** (7), 4358–4368 (2016).
28. Mishra, S. D. & Chakraborty V. and Evaluation of biochemical parameters for screaming resistance of chick-pea cultivars against meloidogyne incognita. *Ind. J. Nematol.* **32** (1), 26–29 (2002).
29. Nikoo, F. S., Sabani, N., Amminian, H., Mukhtarjejadi, L. & Ghaderi, R. Induction of systemic resistance and defense-related enzymes in tomato plants using Pseudomonas fluorescence CHAO and Salicylic acid against root knot nematode meloidogyne incognita. *J. Plant. Prot. Res.* **54**, 4–10 (2014).

30. Ruchi, G. & Singh, S. Study of selected biochemical and physiological changes among the infected by root knot nematode and healthy plants of bitter gourd in four localities at Muzaffarpur. *Indian J. Sci. Res.* **10**, 71 (2020).
31. Hussey, R. S. & Barker, K. R. A comparison of methods of collecting inocula of *Meloidogyne* spp., including a new technique. *Plant. Dis. Reptr.* **57** (12), 1025–1028 (1973).
32. Sun, M. H., Gao, L., Shi, Y. X., Li, B. J. & Liu, X. Z. Fungi and actinomycetes associated with meloidogyne spp. Eggs and females in China and their biocontrol potential. *J. Invertebr. Pathol.* **93** (1), 22–28. https://doi.org/10.1016/j.jip.2006.03.006 (2006).
33. Johansen, D. A. Plant Micro technique. McGraw-Hill, New York, 523 (1940).
34. Bozzola, J. J. & Russell, L. D. *Electron Microscopy Principles and Techniques for Biologists* 41–63 (Jones and Bartlett, 1992).
35. Arnon, D. I. Copper enzymes in isolated chloroplasts. Polyphenoloxidase in beta vulgaris. *Plant. Physiol.* **24** (1), 1–15. https://doi.org/10.1104/pp.24.1.1 (1949).
36. Malick, C. P. & Singh, M. B. Phenolics. In *Plant Enzymology and Histoenzymology* 286 (Kalyani, 1980).
37. Rad, A. M., Ghourchian, H., Moosavi-Movahedi, A. A., Hong, J. & Nazari, K. Spectrophotometric assay for horseradish peroxidase activity based on pyrocatechol-aniline coupling hydrogen donor. *Anal. Biochem.* **362**, 38–43 (2007).
38. Mayer, A. M., Harel, E. & Ben-Shaul, R. Assay of catechol oxidase: critical comparison of methods. *Phytochemistry* **5**, 783–789 (1966).
39. Dickerson, D. P., Pascholati, S. F., Hagerman, A. E., Butler, L. G. & Nicholson, R. L. Phenylalanine ammonia-lyase and hydroxycinnamate: coa ligase in maize mesocotyls inoculated with helminthosporium Maydis or helminthosporium Carbonum. *Physiol. Plant. Pathol.* **25**, 111–123 (1984).
40. Irshad, U. et al. Pathogenicity of citrus nematode (*Tylenchulus semipenetrans*) on *Citrus Jambhiri*. *J. Anim. Plant. Sci.* **22** (4), 1014–1018 (2012).
41. Mukhtar, T., Hussain, M. A., Kayani, M. Z. & Aslam, M. N. Evaluation of resistance to root-knot nematode (*Meloidogyne incognita*) in Okra cultivars. *Crop Prot.* **56**, 25–30. https://doi.org/10.1016/j.cropro.2013.10.019 (2014).

Acknowledgements

The authors are highly thankful to the "Other Backward Classes Cell" (OBC-Cell), University of Mysore, Mysuru, for providing fellowship and the Institution of Excellence (IOE), Vijnana Bhavana, Manasagangotri, Mysuru, for SEM facility. The authors are thankful to Dr. A. Shanthi, Professor and the Department of Nematology, Tamil Nadu Agricultural University (TNAU), Coimbatore – 03, Tamil Nadu, for the training program on Basic Nematological Techniques. The authors are also thankful to the Department of Studies in Botany and the Department of Studies in Biotechnology, Manasagangotri, University of Mysore, Mysuru, Karnataka – 570006.

Author contributions

All authors contributed to the study's conception and design. Material preparation, data collection, and analysis were performed by [Basavaraj V] and [Sharada M S]. The first draft of the manuscript was written by [Basavaraj V], and all authors commented on previous versions. All authors read and approved the final manuscript. We confirm that all authors have read and approved the final version of the manuscript for submission to *Scientific Reports*.

Competing interests

The authors declare no competing interests.

Additional information

Correspondence and requests for materials should be addressed to V.B.